Metabolic Engineering 14 (2012) 91–103

Contents lists available at SciVerse ScienceDirect

Metabolic Engineering

journal homepage: www.elsevier.com/locate/ymben

Dynamic control of gene expression in *Saccharomyces cerevisiae* engineered for the production of plant sesquitepene α-santalene in a fed-batch mode

Gionata Scalcinati [a,1], Christoph Knuf [a,1], Siavash Partow [a], Yun Chen [a], Jérôme Maury [b], Michel Schalk [c], Laurent Daviet [c], Jens Nielsen [a,*], Verena Siewers [a]

[a] Department of Chemical and Biological Engineering, Chalmers University of Technology, SE-412 96 Göteborg, Sweden
[b] Center for Microbial Biotechnology, Department of Systems Biology, Technical University of Denmark, DK-2800 Kgs. Lyngby, Denmark
[c] Firmenich SA, Corporate R&D Division, CH-1211 Geneva 8, Switzerland

ARTICLE INFO

Article history:
Received 2 September 2011
Received in revised form
11 January 2012
Accepted 26 January 2012
Available online 8 February 2012

Keywords:
Metabolic engineering
Isoprenoids
Farnesyl diphosphate
Ergosterol
Squalene synthase
Saccharomyces cerevisiae

ABSTRACT

Microbial cells engineered for efficient production of plant sesquiterpenes may allow for sustainable and scalable production of these compounds that can be used as e.g. perfumes and pharmaceuticals. Here, for the first time a *Saccharomyces cerevisiae* strain capable of producing high levels of α-santalene, the precursor of a commercially interesting compound, was constructed through a rationally designed metabolic engineering approach. Optimal sesquiterpene production was obtained by modulating the expression of one of the key metabolic steps of the mevalonate (MVA) pathway, squalene synthase (Erg9). To couple *ERG9* expression to glucose concentration its promoter was replaced by the *HXT1* promoter. In a second approach, the *HXT2* promoter was used to express an *ERG9* antisense construct. Using the *HXT1* promoter to control *ERG9* expression, it was possible to divert the carbon flux from sterol synthesis towards α-santalene improving the productivity by 3.4 fold. Combining this approach together with the overexpression of a truncated form of 3-hydroxyl-3-methyl-glutaryl-CoA reductase (HMGR) and deletion of lipid phosphate phosphatase encoded by *LPP1* led to a strain with a productivity of 0.18 mg/gDCW h. The titer was further increased by deleting *DPP1* encoding a second FPP consuming pyrophosphate phosphatase yielding a final productivity and titer, respectively, of 0.21 mg/gDCW h and 92 mg/l of α-santalene.

© 2012 Elsevier Inc. All rights reserved.

1. Introduction

The production of plant sesquiterpenes by microbial fermentation is an environmentally friendly and attractive alternative to the commonly used chemical synthesis and plant extraction (Chang and Keasling., 2006; Rohlin et al., 2001; Ajikumar et al., 2008; Kirby and Keasling, 2009, Wang et al., 2011). Sesquiterpenes are mainly used by the chemical industry for production of fragrances and aroma chemicals (Daviet and Schalk, 2010). They represent a diverse class of secondary metabolites, the precursors of which are natively present in the metabolic network of *Saccharomyces cerevisiae* (Förster et al., 2003). Sesquiterpenes are naturally produced in *S. cerevisiae* through the mevalonate (MVA) pathway from multiple condensation of isopentenyl diphosphate (IPP) and dimethyllallyl diphosphate (DMAPP) leading to farnesyl diphosphate (FPP), the universal precursor unit of all sesquiterpenes (C_{15}) (Maury et al., 2005; Withers and Keasling, 2007). Nowadays, most fragrance compounds are produced via plant and microbe extraction (Howes et al., 2004), and by total chemical synthesis or semi-synthesis (Corey et al., 1957; Julia, 1976; Janssens et al., 1992). Traditional methods of extraction are limited by low yields and high costs. Here, microbial biosynthesis offers several advantages: it (i) avoids formation of racemic mixtures providing enantiomerically pure products through enzymatic biocatalysis, (ii) reduces process costs using inexpensive sugar based carbon sources, (iii) increases sustainability avoiding harvesting and extraction from natural sources and thus reducing environmental footprint, (iv) increases yield and productivities using genetic manipulation of the heterologous hosts and (v) is compatible with scalable high density fermentation processes.

α-Santalene is the precursor of α-santalol, one of the main components of East Indian sandalwood oil (Corey et al., 1957; Baldovini et al., 2010). Sandalwood oil is commonly used in cosmetic, perfumery and aromatherapy industries and has recently been identified as a potential chemotherapeutic and chemopreventive agent against skin cancer (Dwivedi et al., 2003). α-santalene is produced enzymatically in a one-step-conversion from farnesol diphosphate catalyzed by a plant santalene synthase (Schalk, 2011). Here, an efficient *S. cerevisiae* strain

* Corresponding author. Fax: +46 31 772 38 01.
E-mail address: nielsenj@chalmers.se (J. Nielsen).
[1] Contributed equally to this research.

1096-7176/$ - see front matter © 2012 Elsevier Inc. All rights reserved.
doi:10.1016/j.ymben.2012.01.007

Nomenclature

FPP	Farnesyl diphosphate
FOH	(*E,E*)-farnesol
SQS	squalene synthase
HMGR	3-hydroxy-3-metyl-glutaryl-coenzyme A reductase
MVA	mevalonate
SanSyn	santalene synthase gene
Log *P*	logarithm (base 10) of partition coefficient

capable of reaching relevant titers and productivities of α-santalene during an optimized fermentation process is constructed. First, yeast was engineered to produce α-santalene by introducing a heterologous santalene synthase gene (*SanSyn*) derived from *Clausena lansium* (wampee) that catalyzes the conversion of FPP to α-santalene (Schalk, 2011). Metabolic engineering has been extensively applied to manipulate metabolic fluxes and enhance the microbial production of sesquiterpene compounds (Ro et al., 2006; Shiba et al., 2007; Takahashi et al., 2007; Asadollahi et al., 2008, 2009, 2010; Kirby et al., 2008; Ma et al., 2011). In order to increase the precursor pool for isoprenoid synthesis enabling efficient conversion to the target compound α-santalene, two of the main regulatory steps of the MVA pathway catalyzed by 3-hydroxyl-3-methyl-glutaryl-CoA reductase (HMGR) and squalene synthase (SQS) were optimized by introducing genetic modifications that enable to channel the flux towards α-santalene synthesis. The conversion of 3-hydroxyl-3-methyl-glutaryl-CoA into mevalonate catalyzed by HMGR is one of the most studied key regulatory steps in the MVA pathway and is considered the main flux controlling step (Scallen and Sanghvi, 1983; Basson et al., 1986). In yeast, two isoforms of HMGR exist encoded by genes *HMG1* and *HMG2* (Basson et al., 1986) and their activity is subject to tight regulation including feedback regulation and cross-regulation (Hampton and Rine, 1994; Hampton et al., 1996; Brown and Goldstein, 1980). HMGR is composed of an interspecies conserved catalytic domain and a variable membrane anchoring region also referred to as sterol sensing domain (SSD). Hmg1 regulation acts at the level of the SSD domain through a complex mechanism leading to protein degradation (Nielsen, 2009). Over-expression of a truncated form of Hmg1 lacking the SSD domain bypasses this post-transcriptional control and results in a constitutively active non-membrane bound form (Donald et al., 1997; Polakowski et al., 1998). This strategy has been extensively used to increase the flow through the MVA pathway in order to produce isoprenoid derived compounds (Jackson et al., 2003; Ro et al., 2006; Kirby et al., 2008; Asadollahi et al., 2009, 2010; Farhi et al., 2011). The second key step in the MVA pathway is represented by SQS, as this controls the flux of FPP towards sterols or non-sterol sesquiterpenes. FPP is a pivotal intermediate as it is a common precursor for production of essential compounds such as dolichol, ubiquinone, isoprenylated proteins and ergosterol (Daum et al., 1998) and its intracellular concentration is tightly regulated at different levels (Goldstein and Brown, 1990). During normal growth conditions, most of the FPP is converted into ergosterol due to the fact that the cellular demand for sterols is greater compared to the demand for non-sterol FPP derived compounds (Kennedy et al., 1999). Strategies to increase sesquiterpene production based on the disruption of the main FPP consuming reaction catalyzed by squalene synthase produced lethal mutants and restoration of viability requires ergosterol supplementation resulting in an economically not feasible process for industrial purposes (Takahashi et al., 2007). Here, we undertook a genetic engineering approach to balance SQS activity during a fermentation process. Previous attempts to control SQS (encoded by *ERG9*) expression diverting the flow from sterol components to desired FPP-derived compounds were mainly based on replacement of the native *ERG9* promoter with the methionine-repressible *MET3* promoter (Ro et al., 2006; Paradise et al., 2008; Asadollahi et al., 2008, 2009, 2010). However, industrial scale development of this system is limited by the cost of the repressor and its possible consumption by the cell. Instead, we aimed at coupling *ERG9* expression to the glucose concentration in the media.

The production capacity of the engineered strains is evaluated through a fermentation process coupling biochemical production to biomass formation that allows capturing the water insoluble compound during production resulting in an efficient *S. cerevisiae* cell factory for biosynthesis of sesquiterpenoid fragrances.

Table 1
S. cerevisiae strains used in this study.

Strain	Genotype	Plasmid	Reference
CEN.PK113-5D	*MAT***a** *MAL2-8^c SUC2 ura3-52*		P. Kötter, University of Frankfurt, Germany
YIP-M0-04	*MAT***a** *MAL2-8^c SUC2 ura3-52* P_{ERG9}Δ::*kanMX*-P_{MET3}		Asadollahi et al., 2008
SCICK00	*MAT***a** *MAL2-8^c SUC2 ura3-52 lpp1*Δ::*loxP* P_{ERG9}Δ::*loxP*-P_{MET3}		This study
SCICK01	*MAT***a** *MAL2-8^c SUC2 ura3-52 lpp1*Δ::*loxP* P_{ERG9}Δ::*loxP*-P_{HXT1}		This study
SCICK03	*MAT***a** *MAL2-8^c SUC2 ura3-52 lpp1*Δ::*loxP* P_{ERG9}Δ::*loxP*-P_{ERG9}		This study
SCICK05	*MAT***a** *MAL2-8^c SUC2 ura3-52 lpp1*Δ::*loxP* P_{ERG9}Δ::*loxP*-P_{ERG9} YMRWdelta15Δ::P_{HXT2}-*ERG9*as-T_{CYC1}-*loxP*		This study
SCICK06	*MAT***a** *MAL2-8^c SUC2 ura3-52*::pSF011-P_{HXT1}		This study
SCICK08	*MAT***a** *MAL2-8^c SUC2 ura3-52*::pSF011-P_{TEF1M2}		This study
SCICK09	*MAT***a** *MAL2-8^c SUC2 ura3-52*::pSF011-P_{HXT2}		This study
SCICK10	*MAT***a** *MAL2-8^c SUC2 ura3-52*::pSF011-P_{MET3}		This study
SCICK11	*MAT***a** *MAL2-8^c SUC2 ura3-52*::pSF011-P_{ERG9}		This study
SCICK12	*MAT***a** *MAL2-8^c SUC2 ura3-52 lpp1*Δ::*loxP* P_{ERG9}Δ::*loxP*-P_{HXT1}	pICK01	This study
SCICK13	*MAT***a** *MAL2-8^c SUC2 ura3-52 lpp1*Δ::*loxP* P_{ERG9}Δ::*loxP*-P_{ERG9}	pICK01	This study
SCICK14	*MAT***a** *MAL2-8^c SUC2 ura3-52 lpp1*Δ::*loxP* P_{ERG9}Δ::*loxP*-P_{ERG9} YMRWdelta15Δ::P_{HXT2}- as*ERG9*-T_{CYC1}-*loxP*	pICK01	This study
SCICK15	*MAT***a** *MAL2-8^c SUC2 ura3-52 lpp1*Δ::*loxP* P_{ERG9}Δ::*loxP*-P_{MET3}	pICK01	This study
SCICK16	*MAT***a** *MAL2-8^c SUC2 ura3-52 lpp1*Δ::*loxP dpp1*Δ::*loxP* P_{ERG9}Δ::*loxP*-P_{HXT1}		This study
SCICK17	*MAT***a** *MAL2-8^c SUC2 ura3-52 lpp1*Δ::*loxP dpp1*Δ::*loxP* P_{ERG9}Δ::*loxP*-P_{HXT1}	pICK01	This study

2. Materials and methods

2.1. Strains and maintenance

Strains used in this study are listed in Table 1. Strains were maintained on YPD plates containing 10 g/l yeast extract, 20 g/l casein peptone, 20 g/l glucose and 20 g/l agar. Plasmid carrying strains were selected on synthetic dextrose (SD) agar containing 6.9 g/l yeast nitrogen base w/o amino acids (Formedium, Hunstanton, UK), 0.77 g/l complete supplement mixture (CSM) w/o uracil (MP Biomedicals, Solon, OH, USA), 20 g/l glucose, and 20 g/l agar and counter-selected on SD plates supplemented with 30 mg/l uracil and 750 mg/l 5-fluoroorotic acid (Formedium). Strains containing the *kanMX* cassette were selected on YPD plates containing 200 mg/l G418 (Formedium).

2.2. Plasmid construction

To construct integrative plasmids carrying the *lacZ* gene under control of different promoters plasmid pSF011 (Partow et al., 2010) was used. Promoters P_{ERG9}, P_{MET3}, P_{HXT1}, and P_{HXT2}, and were PCR amplified from genomic DNA of *S. cerevisiae* CEN.PK113-5D, and P_{TEF1M2} was amplified from plasmid p416TEF1M2 (kindly provided by G. Stephanopoulos, Massachusetts Institute of Technology, Cambridge, MA, USA) using primers 1 to 6 and 50 to 53 (Table 2), restricted with *Not*I/*Hin*dIII and ligated into *Not*I/*Hin*dIII cut pSF011 resulting in formation of plasmids pSF011-P_{ERG9}, pSF011-P_{MET3} and pSF011-P_{HXT1}, pSF011-P_{HXT2} and pSF011-P_{TEF1M2}, respectively.

To construct the α-santalene expression vector the *SanSyn* gene was amplified by PCR from plasmid Cont2B-27-pET101

Table 2
Oligonucleotide primers used in this study[a].

No.	Name	Sequence (5′→3′)
1	HindIII_ERG9_f	CAACAAAAGCTTCCCATCTTCAACAACAATACC
2	NotI_ERG9_r	CAACAAGGCGGCCGCTGTGTGTGTGTGATATGTGACGT
3	HindIII_MET3_f	CAACAAAAGCTTGTATAAGGTGAGGGGGTCCACAG
4	NotI_MET3_r	CAACAAGGCGGCCGCGTTAATTATACTTTATTCTTGTTATTATTATACtttc
5	HindIII_HXT1_f	CAACAAAAGCTTTGCAGGTCTCATCTGGAATATAATTCC
6	NotI_HXT1_r	CAACAAGCGGCCGCGATTTTACGTATATCAACTAGTTGACGATTATqG
7	santa_f	GTTGTTGCGGCCGCAAAACAATGTCAACTCAACAAGTTTCATCAG
8	santa_r	GTTGTTTTAATTAACTAATCGTCAAGCTTAACGGG
9	tHMG1_up	GTTGTTGGATCCAAAACAATGGCTGCAGACCAATTGGTG
10	tHMG1_down	GTTGTTGCTAGCTTAGGATTTAATGCAGGTGACG
11	Int_check_f	GGTTCCGCGCACATTTCCCC
12	Int_check_r	GGAACTCTTGTTGTTCTTTGGAG
13	LacZ_r	GGGATCTGCCATTGTCAGAC
14	LPP_up_f	AAGGATGATCTCTGTCATGG
15	LPP_up_r_tail	GATCCCCGGGAATTGCCATGTGTTAGGGCAGCATTTATGC
16	LPP_dw_f_tail	GCAGGGATGCGGCCGCTGACGCACTCCAAGCGGACATTCAAG
17	LPP_dw_r	GAAGTATGTCTCTTTTCGCC
18	Pr-b-Kan′	CATGGCAATTCCCGGGGATCCCCTTAATATAACTTCGTATAATGTATGC
19	Kan3′int	CCATGAGTGACGACTGAATCCGG
20	Kan5′int	GCAAAGGTAGCGTTGCCAATG
21	dKan3′	GTCAGCGGCCGCATCCCTGCCGACTCACTATAGGGAGACCG
22	LPP1 verif_up	TAGTTGCCACGTGAAACCTGACAAC
23	LPP1 verif_dw	AATTTCATCGGTATTTTGGCTTCGG
24	loxP_ERG9_f	CGAAGTTATTAGGTGATATCAGATCCACTGCCCATCTTCAACAACAATACCG
25	ERG9d_r	GTCGTAGTCGTGGACGGTTTGC
26	loxP_HXT1_f	CGAAGTTATTAGGTGATATCAGATCCACTTGCAGGTCTCATCTGGAATATAATTCC
27	ERG9_Hxt1_r	GCTGCCTTCATCTCGACCGGATGCAATGCCAATTGTAATAGCTTTCCCATGATTTTACGTATATCAACTAGTTGACGATTATG
28	ERG9_loxP_f	GAGTGAACCTGCTGCCTGGCGTGCTCTGACTCAGTACATTTCATAGCCCAGTACGCTGCAGGTCGACAACC
29	loxP_r	AGTGGATCTGATATCACCTAATAACTTCG
30	Erg9_fr_f	CCTTGCTTACACAGAGTGAACCTGCTGCCTGGC
31	Erg9_fr_r	CTTCAGCTTCAAAGCTGCCTTCATCTCGACCG
32	DPP-1-fw	AGGGCACGTTATCAATTGT
33	DPP-1-rev	CAGCGTACGAAGCTTCAGAGAAACTCGTACTGAACCAAG
34	DPP-2-fw	GTGATATCAGATCCACTAGTACAGACATCATTTCGTCGA
35	DPP-2-rev	AACTTCTAAGGCTTTCGTGT
36	KanMx-1-fw	CTGAAGCTTCGTACGCTG
37	KanMx-1-rev	TCACCATGAGTGACGACTGA
38	KanMx-2-fw	TTCCAACATGGATGCTGAT
39	KanMx-2-rev	CTAGTGGATCTGATATCAC
40	Amp_fw	GTGGGTTACATCGAACTGGATC
41	Amp_rv	CATCCATAGTTGCCTGACTGC
42	14up_HXT2_f	GATTTGATGACTGTTTCTCAAAACTTTATGTCATTTTCTTACACCGCATATGATTCTACCGATGTAATACAAAAATG
43	ERG9as_HXT2_r	TTATTGAATTCCACAAATTGAAACTATGTTGCTTTATAAGTCTTTTTGTAA
44	ERG9as_f	GTTTCAATTTGTGGAATTCAATAA
45	CYC1t_ERG9as_r	TTCCTTTTCGGTTAGAGCGGATCTGGAAATTAGGACAGGGGC
46	ERG9as_CYC1t_f	GCCCCTGTCCTAATTTCCAGATCCGCTCTAACCGAAAAGGAA
47	loxP_CYC1t_r	GGTTGTCGACCTGCAGCGTACCTTCGAGCGTCCCAAAACCTT
48	loxP_f	GTACGCTGCAGGTCGACAACC
49	14down_loxP_r	GATAACCGCGAAGATTTATAATGGTTTATCGGTTGCATTTTCCATGAGTAAGTGGATCTGATATCACCTAATAACTTCG
50	HindIII_HXT2_f	CAACAAAAGCTTTTCTACCGATGTAATACAAAAATG
51	NotI_Hxt2_r	CAACAAGGCGGCCGCTATGTTGCTTTATAAGTCTTTTTGTAA
52	HindIIITEF1_M2_f	CAACAAAAGCTTGCACACACCACGGCTCTAAAG
53	NotI_TEF1_M2_r	CAACAAGCGGCCGCTTTTCTAGAAAACTTGGATTAGATTGC

[a] Restriction enzyme recognition sites are underlined.

(Schalk, 2011), using primers 7 and 8, cut with *Not*I/*Pac*I and ligated into *Not*I/*Pac*I restricted vector pSP-G1 (Partow et al., 2010). Subsequently, *tHMG1* was PCR amplified using genomic DNA of *S. cerevisiae* CEN.PK113-5D as template and primers 9 and 10, cut with *Bam*HI/*Nhe*I and ligated into the same vector after restriction with the respective enzymes. This resulted in formation of expression plasmid pICK01.

2.3. Strain construction

Strains carrying a genomic integration of *lacZ* under control of different promoters were constructed by transforming CEN.PK113-5D with the *Nco*I restricted integrative plasmids pSF011-P_{ERG9}, pSF011-P_{MET3}, pSF011-P_{HXT1}, pSF011-P_{HXT2} and pSF011-P_{TEF1M2}, respectively, resulting in formation of strains SCICK11, SCICK10, SCICK06, SCICK09 and SCICK08, respectively. Correct integration at the *ura3-52* locus was verified using primers 11 and 12. To test for tandem integration of the plasmid, primers 11 and 13 were used. To exclude additional integrations of the plasmid, strains were subjected to Southern blot analysis.

The *loxP* flanked *kanMX* cassette in strain YIP-M0-04 was excised with help of the Cre recombinase expression plasmid pSH47 as described by Güldener et al. (1996). To delete *LPP1* in this strain a bipartite gene targeting strategy was applied (Erdeniz et al., 1997). The 5′ and 3′ region of the gene were amplified by PCR using primer pairs 14/15 (fragment 1) and 16/17 (fragment 2), respectively, and genomic DNA of CEN.PK113-5D as template. The 5′ and the 3′ part of the *kanMX* cassette were amplified from plasmid pUG6 (Güldener et al., 1996) using primer pairs 18/19 (fragment 3) and 20/21 (fragment 4), respectively. Complementary primer tails allowed for the combination of fragments 1 and 3 by fusion PCR. Likewise, fragments 2 and 4 were fused to each other. Cells were transformed with both fusion PCR fragments and integration of the *kanMX* cassette at the *LPP1* locus was tested by PCR using primers 22 and 23. Subsequent excision of the *kanMX* cassette led to formation of strain SCICK00.

To replace the *ERG9* controlling *MET3* promoter in SCICK00 the *ERG9* promoter and the *HXT1* promoter were amplified from genomic DNA by PCR using primer pairs 24/25 and 26/27, respectively. In addition, the *kanMX* cassette was amplified in a PCR containing primers 28 and 29. The marker cassette was combined with either of the two promoters by fusion PCR and the resulting fragments were amplified once more using primers 30 and 31 in order to extend the flanking regions for genomic integration. Transformation of SCICK00 with these fragments and subsequent excision of the *kanMX* cassette resulted in strains SCICK01 and SCICK03, respectively.

For genomic integration of an *ERG9* antisense expression cassette, four PCR fragments were generated containing the *HXT2* promoter (primers 42/43, fragment 5), a fragment of *ERG9* (primers 44/45, fragment 6), the *CYC1* terminator (primers 46/47, fragment 7) and the *kanMX* cassette flanked by *loxP* sites (primers 48/49, fragment 8). The *ERG9* fragment comprised the first 412 bp of the coding sequence and 99 bp upstream of the start codon. Fragments 5, 6 and 7 and fragment 7 and 8 were combined by fusion PCR and used to transform SCICK03. 5′ extensions of primers 42 and 49 allowed for integration by homologous recombination at YMRWdelta15 (Flagfeldt et al., 2009). Excision of the *kanMX* cassette resulted in strain SCICK05.

For deletion of *DPP1* in strain SCICK01, bipartite gene targeting was applied as described above. Here, primer pairs 32/33 and 34/35 were used to amplify the 5′ and 3′ region of *DPP1* and primer pairs 36/37 and 38/39 were employed for amplification of the 5′ and 3′ part of the *kanMX* cassette. Integration and following excision of the resistance marker led to formation of strain SCICK16.

By transforming SCICK00, SCICK01, SCICK03, SCICK05 and SCICK16 with plasmid pICK01 strains SCICK15, SCICK12, SCICK13, SCICK14 and SCICK17 were constructed.

2.4. Southern blot analysis

Genomic DNA was cut with *Hin*dIII, separated on a 1% agarose gel and transferred to a Hybond^{TM}-N+ membrane (GE Healthcare, Uppsala, Sweden) according to the supplier's instructions. As probe, a fragment of the ampicillin resistance gene in vector pSF011 was amplified by PCR using primers 40 and 41. The AlkPhos Direct Labeling and Detection system (GE Healthcare) was applied using CDP-*Star* as detection reagent and a ChemiDoc XRS system (Bio-Rad Laboratories, Hercules, CA, USA) for chemiluminescence imaging.

2.5. Media and growth conditions

For batch cultivations, a previously described (Verduyn et al., 1992) mineral salts medium was used consisting of the following (per liter): $(NH_4)_2SO_4$, 5 g; KH_2PO_4, 3 g; $MgSO_4 \cdot 7H_2O$, 0.50 g; Antifoam 289 (A-5551, Sigma-Aldrich, St. Louis, MO, USA), 0.05 ml; trace metals, 1 ml and vitamins, 1 ml. The trace metal solution consisted of the following (per liter): EDTA (sodium salt), 15.0 g; $ZnSO_4 \cdot 7H_2O$, 0.45 g; $MnCl_2 \cdot 2H_2O$, 1 g; $CoCl_2 \cdot 6H_2O$, 0.3 g; $CuSO_4 \cdot 5H_2O$, 0.3 g; $Na_2MoO_4 \cdot 2H_2O$, 0.4 g; $CaCl_2 \cdot 2H_2O$, 0.45 g; $FeSO_4 \cdot 7H_2O$, 0.3 g; H_3BO_3, 0.1 g and KI, 0.1 g. The pH of the trace metal solution was adjusted to 4.0 with 2 M NaOH prior to heat sterilization. The vitamin solution contained (per liter): biotin, 0.05 g; p-amino benzoic acid, 0.2 g; nicotinic acid, 1 g; Ca-pantothenate, 1 g; pyridoxine-HCl, 1 g; thiamine-HCl, 1 g and myo-inositol, 25 g. The pH of the vitamin solution was adjusted to 6.5 with 2 M NaOH. The vitamin solution was filter sterilized and stored at 4 °C. This medium was supplemented with 30 g/l glucose. The medium used for shake flask cultivation had the same composition as described above, but the $(NH_4)_2SO_4$ concentration was increased to 7.5 g/l, and the KH_2PO_4 concentration to 14.4 g/l. The glucose concentration was 20 g/l and the pH was adjusted to 6.5 prior autoclaving. The feed composition used for fed-batch cultivation had the same composition as described above, but the $(NH_4)_2SO_4$; KH_2PO_4; $MgSO_4 \cdot 7H_2O$, vitamin solution, and trace metal solution concentrations were increased 10 times; the glucose concentration was 200 g/l.

2.6. Inoculum preparation

The seed cultures for the cultivations were grown at 30 °C in 500-ml shake flasks containing 100 ml of culture with agitation in an orbital shaker at 100 rpm. Pre-cultures were used to inoculate the fermentors to a final dry weight of 1 mg/l. All cultivations were performed in duplicate.

2.7. Shake flask cultivation

Cultivations were carried out in 500 ml baffled Erlenmeyer flasks with four diametrically opposite baffles and side necks for aseptic sampling. The flasks were prepared with 100 ml medium as described above. Cultures were incubated with agitation in an orbital shaker at 100 rpm and the temperature was controlled at 30 °C.

2.8. Fed-batch mode in shake flasks

Shake flasks in fed-batch mode were realized using the FeedBeads polymer-based slow-release technique as previously described (Jeude et al., 2006). Media were prepared as described

above without initial glucose content. Four sterile silicone elastomer disks Ø12 mm (Kühner AG, Basel, Switzerland) containing glucose crystals were added immediately before inoculation to 250 ml Erlenmeyer flasks containing 25 ml of medium.

2.9. Fed-batch operation

The aerobic fed-batch process was performed in 2.5 l Applikon vessels (Applikon, Schiedam, The Netherlands) with a working volume of 1.0 l. Agitation at 600 rpm was maintained using an integrated stirrer (DasGip, Jülich, Germany) and the temperature kept at 30 °C. The rate of aeration was set to 0.6 l/min. The pH of the medium was maintained at 5.0 by automatic addition of 2 N KOH during the batch phase and 10% NH_4OH during the feed phase. The temperature, agitation, gassing, pH and composition of the off-gas were monitored and controlled using the DasGip monitoring and control system. Dissolved oxygen concentration was monitored with an autoclavable polarographic oxygen electrode (Mettler Toledo, Columbus, OH, USA) and kept above 30% via stirrer speed and gas flow rate using the DasGip control system. The effluent gas from the fermentation was analyzed for real-time determination of oxygen and CO_2 concentration by DasGip fedbatch pro® gas analysis systems with the off gas analyzer GA4 based on zirconium dioxide and two-beam infrared sensor.

The fed-batch cultures were initiated as batch cultures using 30 g/l glucose. Feeding with fresh medium commenced only after residual ethanol produced from the glucose consumption phase was completely depleted. A feed strategy was designed keeping the volumetric growth rate constant (Nielsen et al., 2003). An exponential feed rate $v(t)$ (l/h) was calculated according to:

$$v(t) = \frac{Y_{xs}\mu_0}{s_f - s_0} x_0 V_0 \exp(\mu_0 t)$$

where x_0, s_0 and V_0 were the biomass density (gDCW/l), the substrate concentration (g/l) and the reactor volume (l) at the start of the feed phase, Y_{xs} was the respiratory yield coefficient (g glucose/gDCW); s_f was the concentration of the growth limiting substrate (g glucose/l) in the reservoir; μ_0 the was the specific growth rate (h^{-1}) during the feed phase and t the feeding time. According to the equation above the feed was increased exponentially with a specific feed rate of 0.06 h^{-1}. Correct feed addition was obtained programming the fb-pro software (DasGip) and controlled using the DasGip control system. An organic layer of dodecane (Sigma-Aldrich) was added aseptically to a final volume of 10% (v/v) immediately before starting the feed.

2.10. Analytical methods

The cell dry weight was measured by filtering known volumes of the cultures through pre-dried and pre-weighed 0.45-μm-pores size nitrocellulose filters (Supor-450 membrane filters; PALL Life Sciences Ann Abor, MI). The filters with the biomass were washed with water, dried for 15 min in a microwave oven at 150 W, and weighed again. The optical density at 600 nm was determined using a Hitachi U-1100 spectrophotometer.

Concentrations of glucose, glycerol, ethanol, acetate, succinate and pyruvate were analyzed by an isocratic high-performance liquid chromatography (UltiMate® 3000 Nano, Dionex) with an Aminex HXP-87H ion-exchange column (Bio-Rad, Hercules, CA) at 65 °C using 5 mM H_2SO_4 as mobile phase at a flow rate of 0.6 ml min^{-1}. Glucose, glycerol and ethanol were measured with a refraction index detector (RI-101 Refractive Index Detector, Shodex®), and acetate, succinate and pyruvate were measured with a UV–visible light absorbance detector (UltiMate 3000 Variable Wavelength Detector, Dionex).

2.11. β-Galactosidase activity assay

The enzyme activity assay was performed as described earlier (Flagfeldt et al., 2009).

2.12. Analysis of sesquiterpenes

Sequiterpene production during the course of fermentation was determined as described previously (Asadollahi et al., 2010). Samples from the organic layer were centrifuged 5 min at 5000 g and the supernatants were analyzed by gas chromatography-mass spectrometry (GC/MS) with a DSQ II single quadrupole mass spectrometer (Thermo Scientific, Waltham, MA). Analytes from 1 μL sample were separated on a SLB-5 ms capillary column (15 m, 0.25 mm i.d., 0.25 μm film thickness; Supelco, Bellefonte, PA, USA) using helium as carrier gas at a flow rate of 1.2 ml min^{-1}. A split/splitless injector was used in the splitless mode. The initial oven temperature was 80 °C and the injector temperature was 250 °C. The oven temperature was increased to 120 °C at a rate of 10 °C/min and subsequently increased to 160 °C at a rate of 3 °C/min. The oven temperature was finally increased to 270 °C at a rate of 10 °C/min and held for 5 min at this temperature. Full mass spectra were generated by scanning m/z range within 40–500 for metabolite identification, α-santalene and *E*,*E*-farnesol were identified comparing mass spectra and retention time with the available authentic standards; trans-α-bergamotene by comparison with library spectra using NIST mass spectra search program (http://chemdata.nist.gov/index.html). Quantification of α-santalene and *E*,*E*-farnesol was carried out using standard curves, *trans*-α-bergamotene was quantified with a correction factor determined using α-humulene as internal standard.

2.13. Analysis of total sterol fraction

For the extraction of sterols, a previously described method (Asadollahi et al., 2010) was used with minor modifications. Known volumes of fermentation broth were harvested by centrifuging at 5000 rpm for 10 min. The cell pellet was washed twice with distilled water and the cell suspension was centrifuged for another 10 min at 5000 rpm. The cell pellet was re-suspended in 4 ml of 0.2 N HCl and heated in a water bath at 85 °C for 1 h and then allowed to cool to room temperature. After centrifugation for 10 min at 5000 rpm and removal of the supernatant, the cell pellet was resuspended in 2 ml methanol containing 0.2% (w/v) pyrogallol and 1 ml 4 N KOH and transferred to a 14 ml glass vial sealed with a PTFE lined screw cap, heated again for 2 h in a water bath at 85 °C for saponification and then cooled to room temperature. Sterols were extracted by addition of 5 ml heptane followed by vigorous mixing for 2 min. After 2 h, the *n*-heptane layer was transferred to a new glass vial for HPLC analyses. Quantitative determination of total ergosterol was carried out by a isocratic high-performance liquid cromatograph (UltiMate® 3000 Nano, Dionex) with a reverse phase Develosil column (C30-UG-5; Nomura Chemicals, Aichi, Japan) at 40 °C using 70% MeOH as the mobile phase at a flow rate of 1 ml min^{-1}. The ergosterol concentration was measured with a UV–visible light absorbance detector set at 280 nm (Photodiode Array Detector, Dionex). The amount of ergosterol was determined with Dionex Chromeleon® software using absolute calibration curves.

2.14. Calculation of specific rates and yield coefficients

The maximum specific growth rates, yield coefficients, specific product formation rates and specific substrate consumption rates are expressed as mg or g product substrate per g dry cell weight

per hour and were calculated as previously described (Nielsen et al., 2003) All calculations are limited to the exponential glucose-limited growth phase.

3. Results

3.1. α-Santalene production in S. cerevisiae

The α-santalene production in *S. cerevisiae* was initially evaluated introducing the expression plasmid pICK01 containing a copy of *tHMG1* and santalene synthase (*SanSyn*) under control of the *PGK1* and *TEF1* promoter, respectively, into a *lpp1*Δ strain to reduce farnesol formation (Faulkner et al., 1999) resulting in strain SCICK13. Production capacity was tested cultivating the strain in a batch in situ product removal (ISPR) reactor mode, consisting of an aqueous two-phase partitioning system. This strategy had previously been used successfully to increase product recovery in different microbial production processes (Daugulis, 1991; Stark and von Stockar, 2003). Dodecane was selected as organic phase due to its hydrophobicity (Log $P_{dodecane}$: 6.6; Log $P_{santalene}$: 6.2), low volatility and biocompatibility with *S. cerevisiae* growth (Newman et al., 2006; Asadollahi et al., 2008). Product accumulation in the dodecane layer was monitored by gas chromatography-mass spectrometry (GC/MS). The transformed strain was able to synthesize a low amount of α-santalene. Analysis of the organic layer revealed a major chromatographic peak corresponding in retention time and mass spectrum to the plant-extracted α-santalene and a second minor peak also present in the plant extract, subsequently identified as *trans*-α-bergamotene (Fig. 5). The amount of the sesquiterpenes α-santalene and *trans*-α-bergamotene produced were, respectively, 1.45 ± 0.02 and 0.17 ± 0.01 mg/l.

3.2. MET3 promoter activity during shake flask cultivation

As a next step, we wanted to increase α-santalene production by reducing ergosterol formation. A promoter, which is widely used for lowering the expression of *ERG9* encoding squalene synthase and hereby increasing the FPP pool, is the *MET3* promoter. As mentioned above, this might not be an optimal solution, since the repressing agent, methionine, is metabolized by the cells thus releasing repression. This was demonstrated by fusing P_{MET3} to the *lacZ* gene followed by measuring β-galactosidase activity of the resulting strain (SCICK10) cultivated in shake flasks without L-methionine or supplied with 1 mM and 2 mM L-methionine, respectively. The concentrations of the inhibitor were chosen based on the amounts previously used for *ERG9* repression (Asadollahi et al., 2008). As shown in Fig. 1, the β-galactosidase activity was constant in the cultures not containing L-methionine. In the cultures that contained L-methionine, LacZ activity was initially very low. However, at about mid-exponential phase, it started to increase and rapidly reached the levels measured in the non-repressed culture.

These results thus demonstrate the difficulties controlling promoter activity when the repressing agent is metabolized by the cells. We therefore tested, if D-methionine or 2-hydroxy-4-(methylthio)butyric acid could serve as L-methionine analogs to repress the P_{MET3} promoter, because they may not be metabolized by yeast or metabolized to a lesser extent. At concentrations of up to 4 mM in the medium neither of the two compounds had the capability to reduce P_{MET3} activity (data not shown).

3.3. Evaluation of alternative promoters for controlling squalene synthase activity

Because of the disadvantages of the *MET3* promoter, alternative systems were evaluated to down-regulate *ERG9* expression.

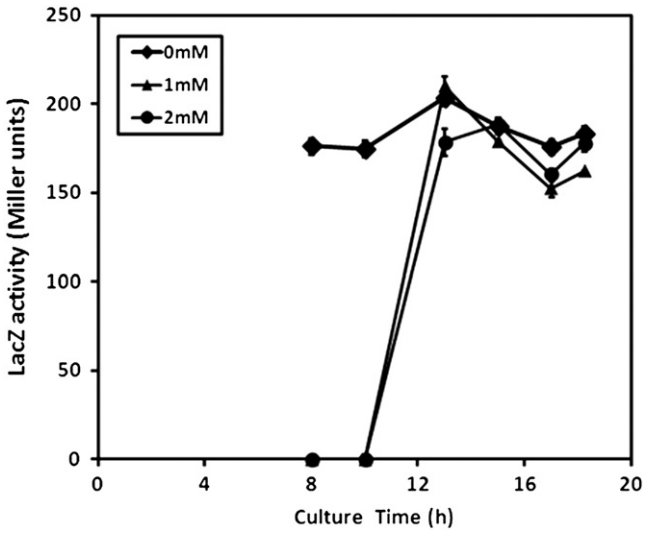

Fig. 1. LacZ activity in strain SCICK10 (P_{MET3}-*lacZ*) in response to different methionine concentrations, 0 mM (diamonds), 1 mM (triangles) and 2 mM (circles). Strains were cultivated in duplicates, glucose exponential growth phase was between 2 and 16 h of cultivation.

The chosen regulatory systems were (i) the low-level constitutive *TEF1* promoter mutant P_{TEF1M2} selected after a directed evolution approach based on error-prone PCR (Alper et al., 2005; Nevoigt et al., 2006), (ii) the glucose concentration controlled promoter of the hexose transporter gene *HXT1* (Ozcan and Johnston, 1995; Lewis and Bisson, 1991) and (iii) the *HXT2* promoter potentially useful for a gene silencing approach expressing *ERG9* antisense mRNA (Ozcan and Johnston, 1995). The approach of using promoters, which are regulated by glucose concentration was chosen as a means to achieve moderate expression levels during exponential growth in batch cultivation, i.e. at high glucose concentration and maximal repression during low glucose concentration, e.g. during the feed phase of a glucose-limited fed-batch process. To test whether the chosen promoters show suitable activity levels compared to the native *ERG9* promoter, fusion constructs of P_{TEF1M2}, P_{HXT1}, P_{HXT2} and P_{ERG9} with the *lacZ* reporter gene were integrated into the yeast genome. Strains SCICK06 (P_{HXT1}), SCICK08 (P_{TEF1M2}), SCICK09 (P_{HXT2}) and SCICK11 (P_{ERG9}) were cultivated in shake flasks and LacZ activity was monitored. Strain SCICK11 showed a steady LacZ activity level throughout the cultivation (Fig. 2). β-galactosidase activity in SCICK06 decreased with decreasing glucose concentration reaching the same level as in SCICK11 in late stationary phase, whereas LacZ activity in SCICK09 increased. During exponential growth, SCICK08 exhibited a very low activity, which increased slightly during stationary phase. The different strains displayed similar growth profiles and no differences were observed in biomass formation.

Developing an efficient cultivation method is a key step in designing a cost effective bioprocess. Fed-batch cultivation mode is widely applied during industrial productions and is often a first choice to achieve high productivity (Nielsen et al., 2003). As previously shown, when controlled by its native promoter, *ERG9* transcript levels display context dependency, i.e. the gene shows different expression levels depending on the growth conditions and the carbon source utilized (Kennedy et al., 1999; Kennedy, 2001). To investigate whether the selected promoters could also be employed during a fed-batch based fermentation process, the same strains were cultivated in the presence of glucose feed beads thus simulating the feed phase in a glucose-limited fed-batch cultivation. Under these conditions, glucose is released

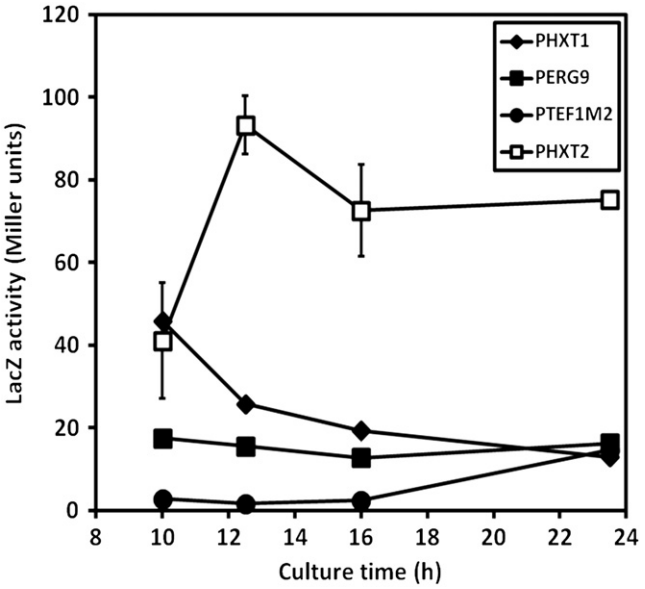

Fig. 2. LacZ activity in strains SCICK06 (P_{HXT1}, filled diamonds), SCICK08 (P_{TEF1M2}, filled circles), SCICK09 (P_{HXT2}, empty squares) and SCICK11 (P_{ERG9}, filled squares) during shake flask cultivation. Strains were cultivated in duplicates, glucose exponential growth phase was between 2 and 16 h of cultivation.

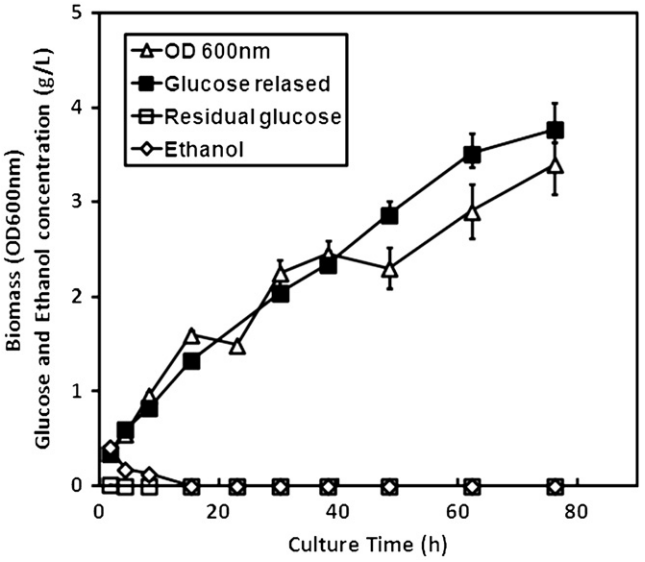

Fig. 3. Shake flask cultivation in fed-batch mode showing absolute glucose release kinetics without cells, residual glucose and ethanol concentration as well as biomass formation. The data represented were obtained for strain SCICK03; all the strains tested exhibited similar profiles.

from silicone elastomers with a controlled kinetics profile (Fig. 3), which allows mimicking a fed-batch fermentation mode comparable to a regular fed-batch. The glucose release (in absence of cells) as well as glucose concentration, cellular growth and by-product formation during the entire cultivation were monitored. This glucose restrained process allows a precise comparison of the different constructs and to fully explore the potential of the glucose sensing promoters. After an initial period of about 5 h of adaptation, where glucose release was larger than the cellular consumption, glucose became the limiting factor for growth and all the glucose released from the elastomers was rapidly converted into biomass with no ethanol overflow metabolism or formation of other by-products (Fig. 3). All strains exhibited a similar growth profile and no significant differences in glucose

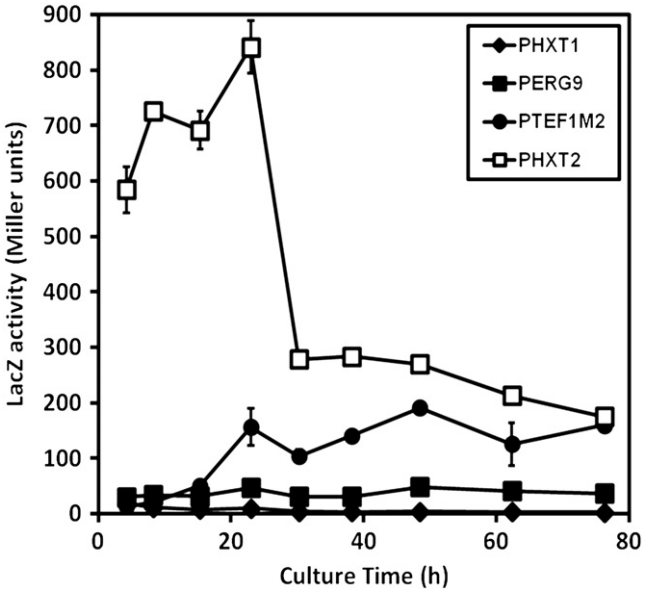

Fig. 4. Characterization of promoter strength during shake flask cultivation in fed-batch mode. β-galactosidase activity in strains SCICK06 (P_{HXT1}, filled diamonds), SCICK08 (P_{TEF1M2}, filled circles), SCICK09 (P_{HXT2}, empty squares) and SCICK11 (P_{ERG9}, filled squares). β-galactosidase activity is the average of values obtained from at least three independent cultivations assayed in duplicates.

consumption (data not shown). The expression of β-galactosidase controlled from the different promoters was assayed at regular intervals and monitored during a cultivation period of 80 h. As in the previous experiment, LacZ activity was steady in SCICK11 (P_{ERG9}) (Fig. 4). As expected, the highest activity was measured for SCICK09 (P_{HXT2}), the lowest for SCICK06 (P_{HXT1}). Surprisingly, β-galactosidase activity in SCICK08 (P_{TEF1M2}) drastically increased during the cultivation finally reaching the same level as for SCICK09 (P_{HXT2}), which indicates that (random) mutagenesis may turn a constitutive promoter – P_{TEF1} had previously shown a constant level of expression throughout different cultivations (Partow et al., 2010) – into a conditional promoter.

According to these results, P_{HXT1} appeared to be a suitable promoter to down-regulate *ERG9* expression under glucose limiting conditions, whereas P_{HXT2} was chosen to regulate the expression of an *ERG9* antisense construct. Due to its high activity levels at low glucose concentrations, the idea of employing P_{TEF1M2} for *ERG9* regulation was discarded.

3.4. Evaluation of santalene production in fed-batch fermentation mode

Based on the results of the promoter characterization study, four strains were constructed. All strains carried a deletion in the phosphatase encoding *LPP1* gene to reduce the loss of FPP to farnesol (Faulkner et al., 1999). *tHMG1* and *SanSyn* were expressed from a high copy number plasmid under control of the *PGK1* and *TEF1* promoter, respectively. Strain SCICK13 containing the native *ERG9* promoter served as a reference strain. In strain SCICK12, the *ERG9* promoter had been replaced by the *HXT1* promoter. Strain SCICK14 carried an antisense DNA fragment comprising the 5′ region of *ERG9* and part of its 5′ UTR (Bonoli et al., 2006; Olsson et al., 1997), whose expression was controlled by the *HXT2* promoter and which was integrated into chromosome XIII at a site providing high expression levels (Flagfeldt et al., 2009). For comparison with previous approaches, strain SCICK15, which carried P_{MET3} instead of P_{ERG9}, was used. In order to maintain *ERG9* repressed in the SCICK15 culture during the

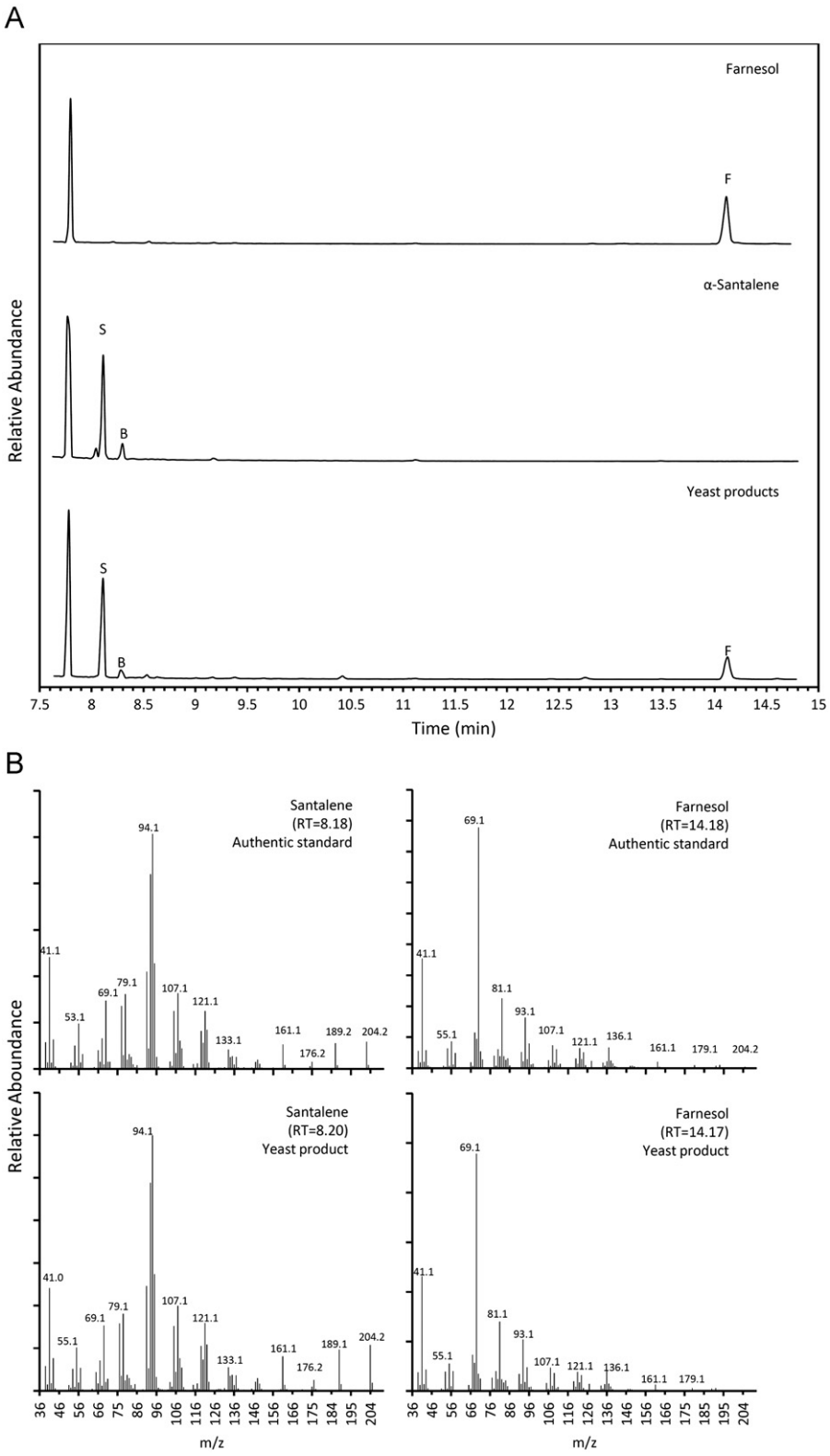

Fig. 5. (A) Total ion chromatograms from GC–MS analysis of authentic standard of farnesol, α-santalene, and an extract of engineered *S. cerevisiae* showing peaks of α-santalene (S), *trans*-α-bergamotene (B) and farnesol (F). The representative ion chromatogram referred to as yeast products was obtained during ISPR fed-batch fermentation of strain SCICK12. (B) Mass spectra and retention times of α-santalene produced from yeast and extracted from plant (left panel) and *E,E*-farnesol produced from yeast and chemical standard (right panel).

fermentation, L-methionine was added at regular intervals every 6 h to a final concentration of 2 mM.

Physiological characterization of the strains was completed in aerobic glucose-limited fed-batch cultures (Table 3). A fed-batch in situ product removal (ISPR) reactor mode was chosen to evaluate the α-santalene production capacity of these strains engineered to accumulate FPP. Cultivation was started as batch with 30 g/l of glucose. After complete glucose consumption and

Table 3
Physiological parameters obtained during fed-batch cultivation of strains SCICK13, SCICK12, SCICK14, SCICK15 and SCICK17.

Strain	μ (h^{-1})	Y_{SX} (g g^{-1})	r_s (mmol (g biomass)$^{-1}$ h^{-1})	r_{CO_2} (mmol (g biomass)$^{-1}$ h^{-1})	r_{O_2} (mmol (g biomass)$^{-1}$ h^{-1})	RQ	Tot_{Sant} (mg l^{-1})
SCICK13 (P_{ERG9})	0.061 ± 0.006	0.50 ± 0.02	0.58 ± 0.03	1.22 ± 0.06	1.29 ± 0.03	0.95 ± 0.01	49.86 ± 0.23
SCICK12 (P_{HXT1})	0.056 ± 0.005	0.50 ± 0.01	0.58 ± 0.02	1.32 ± 0.01	1.43 ± 0.03	0.92 ± 0.01	75.73 ± 0.34
SCICK14 (P_{HXT2})	0.064 ± 0.006	0.48 ± 0.03	0.64 ± 0.28	1.57 ± 0.01	1.62 ± 0.04	0.97 ± 0.01	49.00 ± 0.34
SCICK15 (P_{MET3})	0.057 ± 0.006	0.49 ± 0.03	0.60 ± 0.01	1.49 ± 0.05	1.53 ± 0.07	0.96 ± 0.01	46.56 ± 0.87
SCICK17 (P_{HXT1})	0.057 ± 0.005	0.49 ± 0.01	0.60 ± 0.01	1.46 ± 0.08	1.48 ± 0.09	0.98 ± 0.01	91.96 ± 0.71

Specific growth rate μ (h^{-1}). Biomass yield Y_{SX} (g biomass (g substrate)$^{-1}$). Specific carbon dioxide production rate (r_{CO_2}) and substrate (r_s) and oxygen (r_{O_2}) consumption rates (mmol (g biomass)$^{-1}$ h^{-1}). Respiratory quotient RQ measured as r_{CO_2}/r_{O_2}. Referred to the initial 30 h of the glucose-limited feed phase. Tot_{Sant}, α-santalene titer (mg l^{-1}) measured at the end of the feed process. Values represent the mean ± S.D. of two independent cultivations.

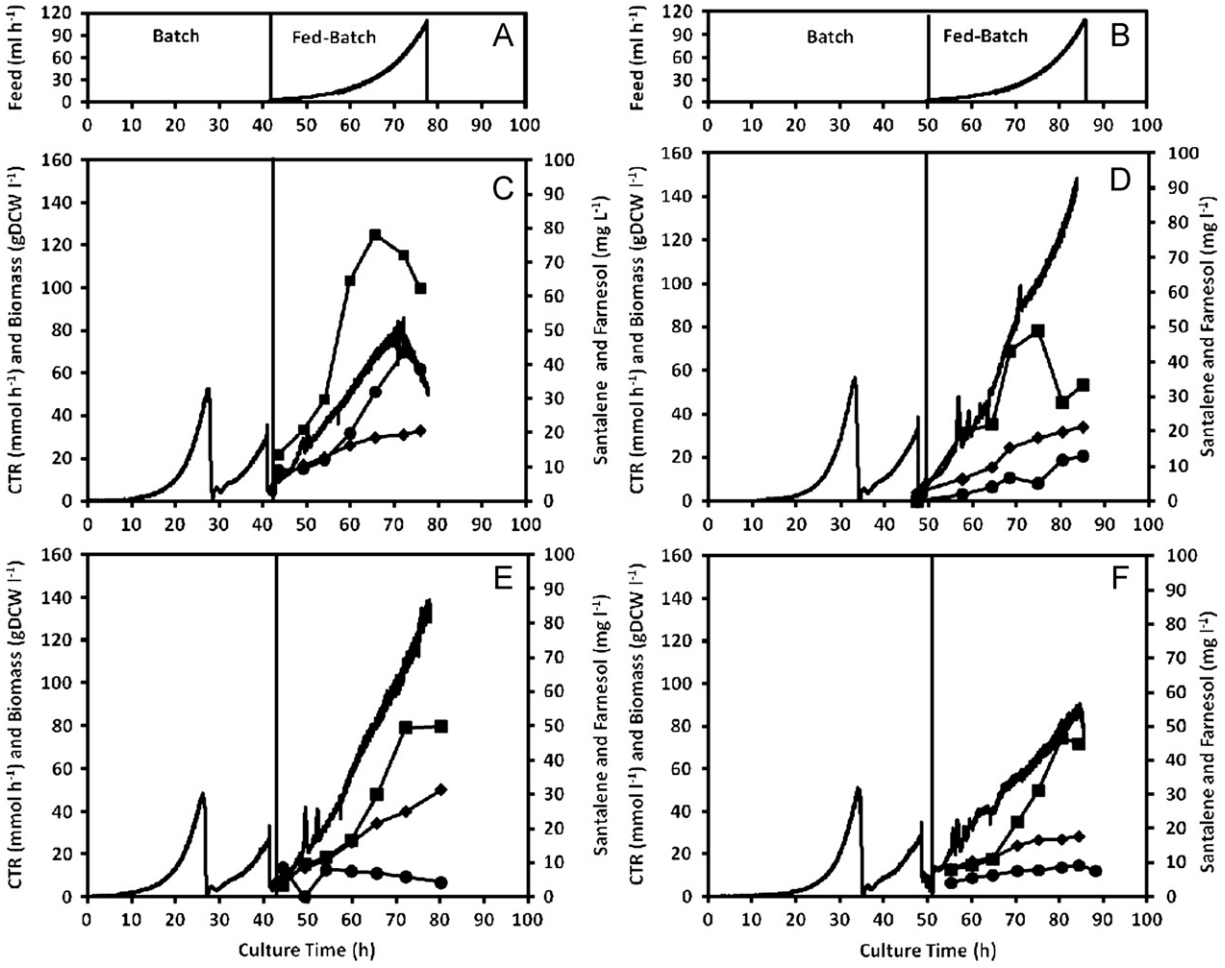

Fig. 6. Time course of an aerobic fed-batch culture with exponential sugar feed of *S. cerevisiae* strains SCICK12 (C) SCKCK14 (D) SCICK13 (E) SCICK15 (F). The feed of glucose (ml h^{-1}) is shown on the upper graph (A) and (B). Typical profile observed for formation of biomass (g l^{-1}, filled diamonds); α-santalene (mg l^{-1}, filled squares); *E,E*-farnesol (mg l^{-1}, filled cycles) carbon dioxide production CTR (mmol h^{-1}, lines) are represented. Data represent the average of two independent cultures.

after residual ethanol produced during the glucose consumption phase was completely depleted, the organic layer was added to the fermentor and the production phase was started by initiating a feed of fresh concentrated substrate with exponential kinetics for a total feed period of 36 h (Fig. 6). Within the first 30 h of feed the culture metabolism was completely respiratory characterized by complete oxidation of glucose with biomass and carbon dioxide as the major products and complete absence of fermentation products, while the respiratory coefficients remained close to 1 for all strains (Table 3). The period of respiratory growth was followed by a phase where yeast growth was no longer consistent with the feeding profile resulting a shift towards fermentative metabolism accompanied by accumulation of glucose and ethanol (data not shown). To examine the effect of *ERG9* repression on the sterol pathway, the total cellular sterol content was measured. Both the two P_{ERG9} replacement mutants and the strain expressing the antisense construct showed a lowered sterol content when compared to the strain containing the original *ERG9* promoter. The decrease in ergosterol ranged from 50 to 91%, and strain SCICK12 (P_{HXT1}) showed the lowest sterol content (Fig. 7).

To establish if the lower sterol content reflected an increased availability of FPP precursor for sesquiterpene conversion, product accumulation in the organic layer was measured. Similarly to the results in shake flasks, formation of α-santalene was accompanied by *trans*-α-bergamotene production observed in

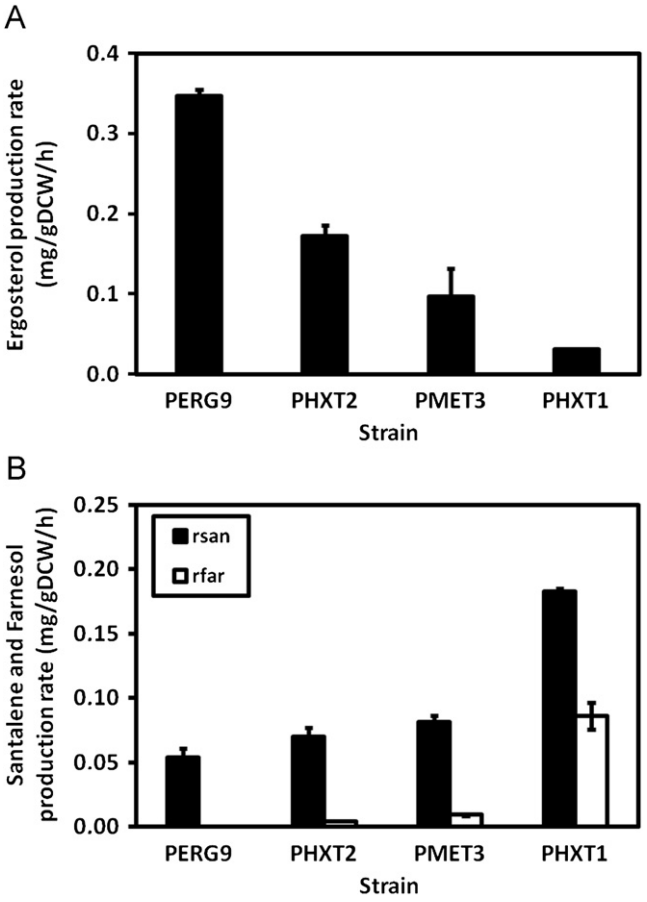

Fig. 7. (A) Ergosterol production rate (mg g biomass^{-1} h^{-1}). (B) α-santalene and *E,E*-farnesol production rate (mg g biomass^{-1} h^{-1}) in strains SCICK13 (P_{ERG9}), SCICK14 (P_{HXT2}-as), SCICK15 (P_{MET3}) and SCICK12 (P_{HXT1}). Strains were grown in a two-phase partitioned fed-batch glucose-limited cultivation mode. The error bars represent the standard deviation for two independent cultivations.

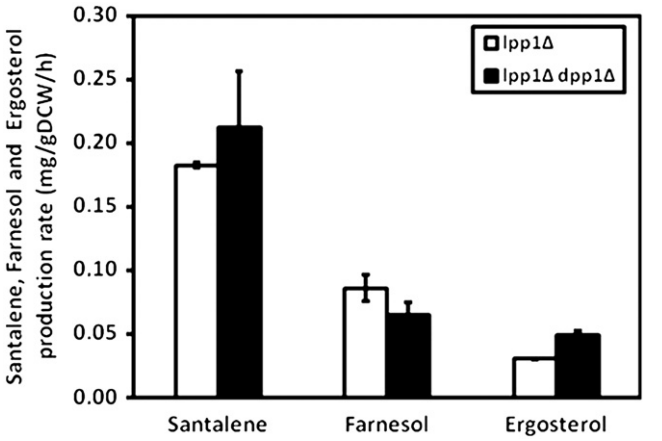

Fig. 8. Effect of single *lpp1*Δ and *lpp1*Δ *dpp1*Δ double deletion on α-santalene, *E,E*-farnesol and ergosterol production rates (mg g biomass^{-1} h^{-1}) in strains SCICK12 (P_{HXT1} *lpp1*Δ) (empty bars) and SCICK17 (P_{HXT1} *lpp1*Δ *dpp1*Δ) (filled bars). The error bars represent the standard deviation for two independent cultivations.

all strains. The amount of *trans*-α-bergamotene detected was proportionally consistent to the amount of α-santalene in all cases and corresponded to about 12% of the total α-santalene produced confirming that this compound is a secondary product of santalene synthase. A linear correlation was observed between the reduction in ergosterol content and the increase in sesquiterpene production. Different levels of *ERG9* repression diverted FPP towards santalene formation redirecting the flux distribution from the sterol pathway to sesquiterpene production with a santalene productivity ranging between 0.054 and 0.183 mg (g biomass)$^{-1}$ h^{-1} (Figs. 6 and 7). Strain SCICK12 (P_{HXT1}) was the best santalene producer with a 3.4 fold improvement in santalene productivity compared to SCICK13 (P_{ERG9}).

As previously described, *ERG9* down-regulation results in accumulation of farnesol (Takahashi et al., 2007; Asadollahi et al., 2008, 2010). Substantial accumulation of farnesol, an FPP-derived by-product, was detected in all strains (Fig. 7). Farnesol formation was inversely correlated with the ergosterol content and correlated to the santalene accumulation pattern observed, suggesting that *ERG9* down-regulation and HMGR over-expression combined with glucose de-repressed growth conditions resulted in an increased availability of FPP for α-santalene synthesis.

3.5. Contribution of DPP1 deletion to santalene production

DPP1 deletion had been used previously in order to reduce farnesol accumulation in a sesquiterpene producing strain (Takahashi et al., 2007). Together with Lpp1, Dpp1 is responsible for most of the cytosolic isoprenoid and lipid phosphate phosphatase activity in *S. cerevisiae* (Toke et al., 1998; Faulkner et al., 1999). As all engineered strains showed an increased conversion of FPP to FOH thus reducing substrate availability for santalene synthase the additional effect of deletion of *DPP1* on the best producing strain SCICK12 (P_{HXT1}) was investigated. *DPP1* was deleted in strain SCICK01 and subsequently transformed with the expression plasmid pICK01 containing a copy of *tHMG1* and santalene synthase resulting in strain SCICK17. Deletion of *DPP1* resulted in an increase of the α-santalene specific production rate from 0.18 to 0.21 mg (g biomass)$^{-1}$ h^{-1} together with a 24% drop in farnesol accumulation, but showed only a minor effect on the ergosterol content (Fig. 8).

Using the different promoter systems, it was possible to increase the santalene productivity from 0.05 to 0.18 mg (g biomass)$^{-1}$ h^{-1}. *DPP1* deletion contributed to reduce the FOH formation and further increase the final santalene titer by 54% (Table 3). Combining these modifications resulted in a strain capable of the highest α-santalene production level of any strain tested with a final titer of 92 mg/liter.

4. Discussion

Previous studies have reported successful examples of expression of different plant derived terpene synthases in the yeast *S. cerevisiae* (Yamano et al., 1994; Jackson et al., 2003; Dejong et al., 2006; Ro et al., 2006; Asadollahi et al., 2008). In this work, yeast was engineered for the first time to produce α-santalene introducing santalene synthase (*SanSyn*) from *C. lansium*. As observed during expression in *Escherichia coli* (Schalk, 2011), α-santalene was the main product formed by this enzyme and only a minor amount of the secondary compound *trans*-α-bergamotene was detected. Catalytic efficiency and specificity of the heterologous synthase are often referred to as key factors in order to achieve relevant titers of the desired compound (Picaud et al., 2005).

Terpene precursors are produced in yeast through the mevalonate pathway (MVA). Due to the variety of essential compounds derived from this pathway, the activity of many enzymes is strictly regulated at different levels (Maury et al., 2005). Yeast was engineered to increase α-santalene production by modulating the expression of two key metabolic steps of the mevalonate pathway (i) down-regulating the squalene synthase gene (*ERG9*)

and (ii) over-expressing the truncated version of HMG-CoA reductase (*tHMG1*) to increase the pool of the critical intermediate FPP and enabling the redirection of the carbon flux towards α-santalene.

FPP-derived squalene is a critical precursor of ergosterol, a key component of the yeast cytoplasmic membrane and essential for membrane fluidity. The attempt to increase the FPP pool by *ERG9* deletion resulted in a complete loss of squalene formation and has been shown to be lethal (Jennings et al., 1991). Ergosterol supplementation for restoring viability would be economically unfeasible for industrial applications. Recently, many different techniques have been applied to reduce a specific gene activity as a suitable alternative to complete gene deletions (Mijakovic et al., 2005; Hammer et al., 2006). In this work, several strategies for down-regulation of *ERG9* were evaluated to precisely adjust enzyme activity throughout the entire course of fermentation enabling sufficient squalene production to fulfill the minimum ergosterol requirements to sustain cellular growth without extracellular sterol supplementation and improve FPP availability for conversion into α-santalene. Characterization of the promoter activity based on a *lacZ* gene reporter assay allowed the identification of promoters that could provide the optimal level of SQS necessary to optimize α-santalene production. Based on their activity profiles, P_{HXT1} and P_{HXT2} were chosen to promote expression of *ERG9* and antisense *ERG9*, respectively, in a fed-batch process with the aim to couple SQS activity to glucose concentration, i.e. to achieve maximal repression during the feed phase when glucose is limiting. Among the different systems tested, repression of *ERG9* transcription under glucose limitation using the P_{HXT1} promoter was more efficient than induction of antisense RNA controlled by P_{HXT2} or employing the previously used P_{MET3} promoter. The minor effect observed using the antisense strategy is probably due to the fact that the expression of asRNA resulted in incomplete gene repression in yeast (Bonoli et al., 2006). Using a glucose responsive promoter has the additional advantage that no addition of an expensive repressing or inducing agent is needed to control its activity.

Data reported in this work show that engineering the FPP branch point increases the cellular pool of FPP reducing the sterol content and leading to an effective enhancement of flux towards sesquiterpenes. Applying different levels of repression of SQS resulted in a consistent redirection of carbon from ergosterol towards α-santalene and FOH. A linear correlation was observed between the different levels of decrease in sterol content and sesquiterpene (santalene+farnesol) formation indicating that down-regulation of *ERG9* changed the availability of FPP and resulted in diverting the flow to the sesquiterpene compounds. It has been hypothesized that SQS has a lower affinity for FPP compared to most of the other enzymes acting at the FPP branch point resulting in high flux toward the non-sterol branches at low FPP concentration (Scheffler, 2002). The catalytic performance of santalene synthase was sufficient to compete with the non-sterol branches and efficiently drained the FPP pool towards the sesquiterpene compound α-santalene. However, santalene synthase was not able to completely convert the excess of FPP and this resulted in accumulation of small amounts of farnesol. This hypothesis was supported by a small increase in the ergosterol level observed when farnesol production was further reduced by deleting *DPP1* leaving the level of α-santalene mainly unchanged. This suggests that the catalytic capacity of santalene synthase could be saturated and therefore not sufficient to convert the additional FPP created by down-regulation of SQS thus resulting in FOH overflow.

Sterol alteration had no effect on the growth characteristics of the engineered strains probably due to the reduced growth rate ($\mu = 0.06 \pm 0.01$) applied during the fed-batch process, which is far below the maximum specific growth rate measured for theses strains under normal batch conditions ($\mu_{max} = 0.35 \pm 0.01$). The accumulation of sterol intermediates is known to result in feedback inhibition of the MVA pathway (Maury et al., 2005). Here, the decrease in sterol content achieved by down-regulating *ERG9* could contribute to relieve this regulatory mechanism and further enrich the flow through the MVA pathway leading to high yields of α-santalene.

According to previous reports, farnesol accumulation was observed in strains over-expressing HMGR (Ohto et al., 2009, 2010). Conversion of FPP to farnesol is the preferred alternative route when squalene synthase is inhibited in mouse, rat and dog (Bansal and Vaidya, 1994). Yeast strains blocked at squalene synthase require ergosterol for growth and produce farnesol (Song, 2003). FOH accumulation was previously detected in yeast strains treated with zaragozic acid, a natural inhibitor of SQS (Kuranda et al., 2010). Moreover, the acitivity of HMGR is increased in glucose de-repressed fermentation mode (Quain and Haslam, 1979). Farnesol formation could be explained by the effects of the deregulation of HMGR combined with glucose de-repressed growth conditions that increased the intracellular FPP concentration and shunted the FPP pool towards farnesol via dephosphorylation. Due to the potentially toxic effect of intracellular FPP accumulation (Bansal and Vaidya., 1994), dephosphorylation could act as self-defense mechanism diverting the excess of FPP into FOH that can then be secreted.

In contrast to other organisms where farnesol production is attributed to specific farnesyl pyrophosphatases (Christophe and Popja, 1961; Bansal and Vaidya, 1994), yeast enzymatic activities involved in the FPP dephosphorylation process have not been fully elucidated yet. Several mechanisms have been suggested, among them (i) self-de-phosphorylation by FPP synthase (Erg20) (Chambon et al., 1990); (ii) non-identified specific phosphatase or pyrophospatase activities (Chambon et al., 1990) and (iii) acid catalyzed non-enzymatic hydrolysis (Muramatsu et al., 2008). Biochemical enzymatic characterizations demonstrated that diacylglycerol pyrophosphate phosphatase encoded by *DPP1* has broad substrate specificity and can utilize isoprenoid phosphate compounds as substrate (Faulkner et al., 1999; Carman and Wu, 2007). Deletion of *DPP1* has been previously used in an attempt to reduce dephosphorylation of FPP to FOH during isoprenoid production resulting in a reduction of 67% in the FOH production from 90 mg/l to 30 mg/l (Takahashi et al., 2007). Together with Dpp1, lipid phosphate phosphatase Lpp1 accounts for most of the cytosolic lipid phosphate phosphatase activity in *S. cerevisiae* (Toke et al., 1998). When two enzymes compete for the same substrate the catalytic efficiency (V_{max}/K_m) may represent a decisive parameter for increasing the flux through a specific enzyme. Previous work showed that simultaneous knock-out of *LPP1* and *DPP1* reduced the rate of hydrolysis of FPP into FOH in vitro to about 10% (Faulkner et al., 1999). Introducing *DPP1* deletion in an *lpp1*Δ strain further improved α-santalene productivity in the fermentation process at the expense of FOH formation.

An efficient fermentation process strategy that couples biochemical production to biomass formation was utilized for improving the production of α-santalene. Fed-batch fermentation operations are commonly used during industrial production processes to achieve a high yield and productivity of the target product (Nielsen et al., 2003). Limited exponential feed profiles of glucose for *S. cerevisiae* fed-batch cultivations were used to maximize the carbon flux from glucose to biomass and the desired target compound, alleviating glucose repression and Crabtree effect (Pronk et al., 1996). Due to the low water solubility of α-santalene the compound easily gets stripped with the gas bubbles used for aeration, but here the product was

captured using an in situ product removal bioreactor set-up. This technique has been intensively used to enhance the production of high value products such as secondary metabolites (Daugulis, 1997). This double phase partitioning system allows an in situ product capturing in the bioreactor minimizing loss of volatiles and compounds with low solubility through the gas outlet and reducing potential toxic effect due to product accumulation.

Combining a metabolic engineering strategy together with fermentation optimization, a production process capable of reaching industrial relevant amounts of the compound α-santalene was realized. Final titers of approximately 92 mg l^{-1} and 131 mg l^{-1} of α-santalene and total sequiterpene were reached in 36 h of feed from a synthetic minimal medium. Furthermore, our study shows that through the use of glucose concentration regulated promoters it is possible to dynamically redirect carbon fluxes in the cell during fed-batch fermentation, and this approach may find application also in the production of a wide range of other products by yeast.

Acknowledgments

Part of this work has been financed by the Knut and Alice Wallenberg Foundation and the Chalmers Foundation. The authors would like to thank Anne Pedersen for her valuable assistance in the strain construction.

References

Ajikumar, P.K., Tyo, K., Carlsen, S., Mucha, O., Phon, T.H., Stephanopoulos, G., 2008. Terpenoids: opportunities for biosynthesis of natural product drugs using engineered microorganisms. Mol. Pharmacol. 5, 167–190.

Alper, H., Fischer, C., Nevoigt, E., Stephanopoulos, G., 2005. Tuning genetic control through promoter engineering. Proc. Natl. Acad. Sci. USA 102, 12678–12683.

Asadollahi, M.A., Maury, J., Møller, K., Nielsen, K.F., Schalk, M., Clark, A., Nielsen, J., 2008. Production of plant sesquiterpenes in *Saccharomyces cerevisiae*: effect of *ERG9* repression on sesquiterpene biosynthesis. Biotechnol. Bioeng. 99, 666–677.

Asadollahi, M., Maury, J., Patil, K.R., Schalk, M., Clark, A., Nielsen, J., 2009. Enhancing sesquiterpene production in *Saccharomyces cerevisiae* through *in silico* driven metabolic engineering. Metab. Eng. 11, 328–334.

Asadollahi, M.A., Maury, J., Schalk, M., Clark, A., Nielsen, J., 2010. Enhancement of farnesyl diphosphate pool as direct precursor of sesquiterpenes through metabolic engineering of the mevalonate pathway in *Saccharomyces cerevisiae*. Biotechnol. Bioeng. 106, 86–96.

Baldovini, N., Delasalle, C., Joulain, D., 2010. Phytochemistry of the heartwood from fragrant *Santalum* species: a review. Flavour Fragr. J. 26, 7–26.

Bansal, V.S., Vaidya, S., 1994. Characterization of two distinct allyl pyrophosphatase activities from rat liver microsomes. Arch. Biochem. Biophys. 315, 393–399.

Basson, M.E., Thorsness, M., Rine, J., 1986. *Saccharomyces cerevisiae* contains two functional genes encoding 3-hydroxy-3-methylglutaryl-coenzyme A reductase. Proc. Natl. Acad. Sci. USA 83, 5563–5567.

Bonoli, M., Graziola, M., Poggi, V., Hochkoeppler, A., 2006. RNA complementary to the 5′ UTR of mRNA triggers effective silencing in *Saccharomyces cerevisiae*. Biochem. Biophys. Res. Commun. 339, 1224–1231.

Brown, M.S., Goldstein, J.L., 1980. Multivalent feedback regulation of HMG CoA reductase, a control mechanism coordinating isoprenoid synthesis and cell growth. J. Lipid Res. 21, 505–517.

Carman, G.M., Wu, W.I., 2007. Lipid phosphate phosphatases from *Saccharomyces cerevisiae*. Methods Enzymol. 434, 305–315.

Chambon, C., Ladeveze, V., Oulmouden, A., Servouse, M., Karst, F., 1990. Isolation and properties of yeast mutants affected in farnesyl diphosphate synthetase. Curr. Genet. 18, 41–46.

Chang, M.C., Keasling, J.D., 2006. Production of isoprenoid pharmaceuticals by engineered microbes. Nat. Chem. Biol. 2, 674–681.

Christophe, J., Popja, G., 1961. Study on biosynthesis of cholesterol: XIV. The origin of prenoic acids from allyl pyrophosphates in liver enzyme systems. J. Lipid Res. 2, 244–257.

Corey, E.J., Chow, S.W., Scherrer, R.A., 1957. The synthesis of α-santalene and of *trans*-$\Delta^{11,12}$-iso-α-santalene. J. Am. Chem. Soc. 79, 5773.

Daugulis, A.J., 1991. Integrated product formation and recovery. Curr. Opin. Biotechnol. 2, 408–412.

Daugulis, A.J., 1997. Partitioning bioreactors. Curr. Opin. Biotechnol. 8, 169–174.

Daum, G., Lees, N.D., Bard, M., Dickson, R., 1998. Biochemistry, cell biology and molecular biology of lipids of *Saccharomyces cerevisiae*. Yeast 14, 1471–1510.

Daviet, L., Schalk, M., 2010. Biotechnology in plant essential oil production: progress and perspective in metabolic engineering of the terpene pathway. Flavour Fragr. J. 25, 123–127.

Dejong, J.M., Liu, Y., Bollon, A.P., Long, R.M., Jennewein, S., Williams, D., Croteau, R.B., 2006. Genetic engineering of taxol biosynthetic genes in *Saccharomyces cerevisiae*. Biotechnol. Bioeng. 93, 212–224.

Donald, K.A., Hampton, R.Y., Fritz, I.B., 1997. Effects of overproduction of the catalytic domain of 3-hydroxy-3-methylglutaryl coenzyme A reductase on squalene synthesis in *Saccharomyces cerevisiae*. Appl. Environ. Microbiol. 63, 3341–3344.

Dwivedi, C., Guan, X., Harmsen, W.L., Voss, A.L., Goetz-Parten, D.E., Koopman, E.M., Johnson, K.M., Valluri, H.B., Matthees, D.P., 2003. Chemopreventive effects of alpha-santalol on skin tumor development in CD-1 and SENCAR mice. Cancer Epidemiol. Biomarkers Prev. 12, 151–156.

Erdeniz, N., Mortensen, U.H., Rothstein, R., 1997. Cloning-free PCRbased allele replacement methods. Genome Res. 7, 1174–1183.

Farhi, M., Marhevka, E., Masci, T., Marcos, E., Eyal., Y., Ovadis, M., Abeliovich, H., Vainstein, A., 2011. Harnessing yeast subcellular compartments for the production of plant terpenoids. Metab. Eng. 13, 474–481.

Faulkner, A., Chen, X., Rush, J., Horazdovsky, B., Waechter, C.J., Carman, G.M., Sternweis, P.C., 1999. The *LPP1* and *DPP1* gene products account for most of the isoprenoid phosphate phosphatase activities in *Saccharomyces cerevisiae*. J. Biol. Chem. 274, 14831–14837.

Flagfeldt, D.B., Siewers, V., Huang, L., Nielsen, J., 2009. Characterization of chromosomal integration sites for heterologous gene expression in *Saccharomyces cerevisiae*. Yeast 26, 545–551.

Förster, J., Famili, I., Fu, P., Palsson, B.Ø., Nielsen, J., 2003. Genome-scale reconstruction of the *Saccharomyces cerevisiae* metabolic network. Genome Res. 13, 244–253.

Goldstein, J.L., Brown, M.S., 1990. Regulation of the mevalonate pathway. Nature 343, 425–430.

Güldener, U., Heck, S., Fiedler, T., Beinhauer, J., Hegemann, J.H., 1996. A new efficient gene disruption cassette for repeated use in budding yeast. Nucleic Acids Res. 24, 2519–2524.

Hammer, K., Mijakovic, I., Jensen, P.R., 2006. Synthetic promoter libraries-tuning of gene expression. Trends Biotechnol. 24, 53–55.

Hampton, R.Y., Rine, J., 1994. Regulated degradation of HMG-CoA reductase, an integral membrane protein of the endoplasmic reticulum, in yeast. J. Cell Biol. 125, 299–312.

Hampton, R., Dimster-Denk, D., Rine, J., 1996. The biology of HMG-CoA reductase: the pros of contra-regulation. Trends Biochem. Sci. 21, 140–145.

Howes, M.J., Simmonds, M.S., Kite, G.C., 2004. Evaluation of the quality of sandalwood essential oils by gas chromatography-mass spectrometry. J. Chromatogr. A 1028, 307–312.

Jackson, B.E., Hart-Wells, E.A., Matsuda, S.P., 2003. Metabolic engineering to produce sesquiterpenes in yeast. Org. Lett. 5, 1629–1632.

Janssens, L., De Pooter, H.L., Shamp, N.M., Vandamme, E.J., 1992. Production of flavours by microorganisms. Process Biochem. 27, 195–215.

Jennings, S.M., Tsay, Y.H., Fisch, T.M., Robinson, G.W., 1991. Molecular cloning and characterization of the yeast gene for squalene synthetase. Proc. Natl. Acad. Sci. USA 88, 6038–6042.

Jeude, M., Dittrich, B., Niederschulte, H., Anderlei, T., Knocke, C., Klee, D., Büchs, J., 2006. Fed-batch mode in shake flasks by slow-release technique. Biotechnol. Bioeng. 95, 433–445.

Julia, M., 1976. Process for Synthesizing Cis-α-Santalene and Cis-α-Santalol. US Patent No. 3970706.

Kennedy, M.A., Barbuch, R., Bard, M., 1999. Transcriptional regulation of the squalene synthase gene (*ERG9*) in the yeast *Saccharomyces cerevisiae*. Biochim. Biophys. Acta 1445, 110–122.

Kennedy, M.A., 2001. Positive and negative regulation of squalene synthase (*ERG9*), an ergosterol biosynthetic gene, in *Saccharomyces cerevisiae*. Biochem. Biophys. Acta 1517, 177–189.

Kirby, J., Romanini, D.W., Paradise, E.M., Keasling, J.D., 2008. Engineering triterpene production in *Saccharomyces cerevisiae*—beta-amyrin synthase from *Artemisia annua*. FEBS J. 275, 1852–1859.

Kirby, J., Keasling, J.D., 2009. Biosynthesis of plant isoprenoids: perspectives for microbial engineering. Annu. Rev. Plant Biol. 60, 335–355.

Kuranda, K., François, J., Palamarczyk, G., 2010. The isoprenoid pathway and transcriptional response to its inhibitors in the yeast *Saccharomyces cerevisiae*. FEMS Yeast Res. 10, 14–27.

Lewis, D.A., Bisson, L.F., 1991. The *HXT1* gene product of *Saccharomyces cerevisiae* is a new member of the family of hexose transporters. Mol. Cell. Biol. 11, 3804–3813.

Ma, S.M., Garcia, D.E., Redding-Johanson, A.M., Friedland, G.D., Chan, R., Batth, T.S., Haliburton, J.R., Chivian, D., Keasling, J.D., Petzold, C.J., Lee, T.S., Chhabra, S.R., 2011. Optimization of heterologous mevalonate pathway through the use of variant HMG-CoA reductases. Metab. Eng. 13, 588–597.

Maury, J., Asadollahi, M.A., Møller, K., Clark, A., Nielsen, J., 2005. Microbial isoprenoid production: an example of green chemistry through metabolic engineering. Adv. Biochem. Eng. Biotechnol. 100, 19–51.

Mijakovic, I., Petranovic, D., Jensen, P.R., 2005. Tunable promoters in systems biology. Curr. Opin. Biotechnol. 16, 329–335.

Muramatsu, M., Ohto, C., Obata, S., Sakuradani, E., Shimizu, S., 2008. Various oils and detergents enhance the microbial production of farnesol and related prenyl alcohols. J. Biosci. Bioeng. 106, 263–267.

Nevoigt, E., Kohnke, J., Fischer, C.R., Alper, H., Stahl, U., Stephanopoulos, G., 2006. Engineering of promoter replacement cassettes for fine-tuning of gene expression in *Saccharomyces cerevisiae*. Appl. Environ. Microbiol. 72, 5266–5273.

Newman, J.D., Marshall, J., Chang, M., Nowroozi, F., Paradise, E., Pitera, D., Newman, K.L., Keasling, J.D., 2006. High-level production of amorpha-4,11-diene in a two-phase partitioning bioreactor of metabolically engineered *Escherichia coli*. Biotechnol. Bioeng. 95, 684–691.

Nielsen, J., Villadsen, J., Liden, G., 2003. Bioreaction Engineering Principles, second ed. Kluywer Plenum, New York.

Nielsen, J., 2009. Systems biology of lipid metabolism: from yeast to human. FEBS Lett. 583, 3905–3913.

Ohto, C., Muramatsu, M., Obata, S., Sakuradani, E., Shimizu, S., 2009. Overexpression of the gene encoding HMG-CoA reductase in *Saccharomyces cerevisiae* for production of prenyl alcohols. Appl. Microbiol. Biotechnol. 82, 837–845.

Ohto, C., Muramatsu, M., Obata, S., Sakuradani, E., Shimizu, S., 2010. Production of geranylgeraniol on overexpression of a prenyl diphosphate synthase fusion gene in *Saccharomyces cerevisiae*. Appl. Microbiol. Biotechnol. 87, 1327–1334.

Olsson, L., Larsen, M.E., Rønnow, B., Mikkelsen, J.D., Nielsen, J., 1997. Silencing *MIG1* in *Saccharomyces cerevisiae*: effects of antisense *MIG1* expression and *MIG1* gene disruption. Appl. Environ. Microbiol. 63, 2366–2371.

Ozcan, S., Johnston, M., 1995. Three different regulatory mechanisms enable yeast hexose transporter (*HXT*) genes to be induced by different levels of glucose. Mol. Cell. Biol. 15, 1564–1572.

Paradise, E.M., Kirby, J., Chan, R., Keasling, J.D., 2008. Redirection of flux through the FPP branch-point in *Saccharomyces cerevisiae* by down-regulating squalene synthase. Biotechnol. Bioeng. 100, 371–378.

Partow, S., Siewers, V., Bjørn, S., Nielsen, J., Maury, J., 2010. Characterization of different promoters for designing a new expression vector in *Saccharomyces cerevisiae*. Yeast 27, 955–964.

Picaud, S., Olofsson, L., Brodelius, M., Brodelius, P.E., 2005. Expression, purification, and characterization of recombinant amorpha-4,11-diene synthase from *Artemisia annua* L. Arch. Biochem. Biophys. 436, 215–226.

Polakowski, T., Stahl, U., Lang, C., 1998. Overexpression of a cytosolic hydroxymethylglutaryl-CoA reductase leads to squalene accumulation in yeast. Appl. Microbiol. Biotechnol. 49, 66–71.

Pronk, J.T., Steensma, H., van Dijken, J.P., 1996. Pyruvate metabolism in *Saccharomyces cerevisiae*. Yeast 12, 1607–1633.

Quain, D.E., Haslam, J.M., 1979. The effects of catabolite derepression on the accumulation of steryl esters and the activity of p-hydroxymethylglutaryl-CoA reductase in *Saccharomyces cerevisiae*. J. Gen. Microbiol. 111, 343–351.

Ro, D.K., Paradise, E.M., Ouellet, M., Fisher, K.J., Newman, K.L., Ndungu, J.M., Ho, K.A., Eachus, R.A., Ham, T.S., Kirby, J., Chang, M.C.Y., Withers, S.T., Shiba, Y., Sarpong, R., Keasling, K.D., 2006. Production of the anitmalarial drug precursor artemisinic acid in engineered yeast. Nature 440, 940–943.

Rohlin, L., Oh, M.K., Liao, J.C., 2001. Microbial pathway engineering for industrial processes: evolution, combinatorial biosynthesis and rational design. Curr. Opin. Microbiol. 4, 330–335.

Scallen, T.J., Sanghvi, A., 1983. Regulation of three key enzymes in cholesterol metabolism by phosphorylation/dephosphorylation. Proc. Natl. Acad. Sci. USA 80, 2477–2480.

Schalk, M., 2011. Method for Producing Alpha-Santalene. US Pat 2011/008836 A1.

Scheffler, I.E., 2002. Metabolic Pathways Inside Mitochondria, in Mitochondria. John Wiley & Sons, Inc., New York (pp. 298–344).

Shiba, Y., Paradise, M.E., Kirby, J., Ro, K.D., Keasling, D.J., 2007. Engineering of the pyruvate dehydrogenase bypass in *Saccharomyces cerevisiae* for high-level production of isoprenoids. Metab. Eng. 9, 160–168.

Song, L., 2003. Detection of farnesyl diphosphate accumulation in yeast *ERG9* mutants. Anal. Biochem. 317, 180–185.

Stark, D., von Stockar, U., 2003. In situ product removal (ISPR) in whole cell biotechnology during the last twenty years. Adv. Biochem. Eng./Biotechnol. 80, 150–175.

Takahashi, S., Yeo, Y., Greenhagen, B.T., McMullin, T., Song, L., Maurina-Brunker, J., Rosson, R., Noel, J.P., Chappell, J., 2007. Metabolic engineering of sesquiterpene metabolism in yeast. Biotechnol. Bioeng. 97, 170–181.

Toke, D.A., Bennett, W.L., Dillon, D.A., Wu, W.I., Chen, X., Ostrander, D.B., Oshiro, J., Cremesti, A., Voelker, D.R., Fischl, A.S., Carman, G.M., 1998. Isolation and characterization of the *Saccharomyces cerevisiae DPP1* gene encoding diacylglycerol pyrophosphate phosphatase. J. Biol. Chem. 273, 3278–3284.

Verduyn, V., Postma, E., Scheffers, W.A., Van Dijken, J.P., 1992. Effect of benzoic acid on metabolic fluxes in yeasts: a continuous-culture study on the regulation of respiration and alcoholic fermentation. Yeast 8, 501–517.

Wang, C., Yoon, H.S., Jang, J.H., Chung, R.Y., Kim, Y.J., Choi, S.E., Kim, W.S., 2011. Metabolic engineering of *Escherichia coli* for α-farnesene production. Metab. Eng. doi:10.1016/j.ymben.2011.08001.

Withers, S.T., Keasling, J.D., 2007. Biosynthesis and engineering of isoprenoid small molecules. Appl. Microbiol. Biotechnol. 73, 980–990.

Yamano, S., Ishii, T., Nakagawa, M., Ikenaga, H., Misawa, N., 1994. Metabolic engineering for production of beta-carotene and lycopene in *Saccharomyces cerevisiae*. Biosci. Biotechnol. Biochem. 58, 1112–1114.